Contents of the Supplement

Supplementary Tables

Table S1. Basic statistics of selected hydrological and meteorological parameters in the study area during the sampling period (October 2022–October 2023).

Parameter	Unit	Statistic	Value	Date
Dunajec River flow rate	$m^3 s^{-1}$	Mean	80.55	-
		Min	20.90	30.11.2022
		Max	472.00	07.08.2023
Dunajec River water level	m asl	Mean	189.00	-
		Min	188.47	31.10.2022
		Max	191.27	07.08.2023
Air temperature	°C	Mean	10.79	-
		Min	-5.6	19.12.2022
		Max	26.7	16.07.2023
Relative air humidity	%	Mean	77.06	-
		Min	41.6	18.03.2023
		Max	99.6	23.01.2023
Precipitation	mm	Mean	2.19	-
		Max	38.5	17.07.2023
		Sum	804.9	-

Dunajec river flow rate measured at the Zgłobice water-gauging station (Fig. 2). Dunajec River water level measured at the surface water intake (Fig. 1). Weather data measured at the Tarnów station (Fig. 2). Source of the data: Dunajec flow rate and weather data: IMWM-NRI (2024), Dunajec water level: this study. Min – Minimum; Max – Maximum.

Table S2. Description of the datasets analysed in the study.

Dataset	Dataset description	Source
Field $\delta^{18}O$, $\delta^{2}H$ and Cl^{-} measurements in surface water and groundwater in the Kępa Bogumiłowicka RBF site region	Monthly data on $\delta^{18}O$, $\delta^{2}H$ and Cl^{-}, measured in the Dunajec River, four production wells (S31, S36, S37, S39) and the observation well E1 from 10.2022 to 10.2023 ($\delta^{18}O$ and $\delta^{2}H$) and 01.2023 to 10.2023 (Cl^{-}).	Fieldwork of this study
Field high-resolution water level, temperature, and SC measurements	High-resolution data on water level, temperature, and SC in the Dunajec River, four production wells (S31, S36, S37, S39) and the observation well E1.	
Archival $\delta^{18}O$ and $\delta^{2}H$ measurements in surface water, groundwater and precipitation	$\delta^{18}O$ in the Dunajec River: Nowy Targ: June 2016 (n = 2, source: Kotowski et al., 2023); Červený Kláštor: April 1982, April 1992, March 1993, and August 2013 (n = 4, source: Bodiš et al., 2015). $\delta^{18}O$ in the Poprad River: Spišská Teplica and Plaveč: three measurements in April 1982, April 1992, and March 1993; Kežmarok: one measurement in March 1993; Chmeľnica: one measurement in August 2013 (source: Bodiš et al., 2015). $\delta^{2}H$ in the Dunajec River: Nowy Targ: mean from two measurements in June 2016 (source: Kotowski et al., 2023); Červený Kláštor: one measurement in August 2013 (source: Bodiš et al., 2015). $\delta^{2}H$ in the Poprad River: Chmeľnica: one measurement in August 2013 (source: Bodiš et al., 2015).	Bodiš et al. (2015) Kotowski et al. (2023)
	Data on $\delta^{18}O$ and $\delta^{2}H$ in recent (age to c. -60 years) Quaternary groundwaters in southern Poland were measured at various frequencies.	PGI-NRI (2024)
	Monthly data on $\delta^{18}O$ and $\delta^{2}H$ in precipitation from the Kraków (2000–2023), Liesek (1988–1995), Stara Lesna (1988–1995) and Ornak (1984–1985) stations.	IAEA/WMO (2024) Różański and Duliński (1988)
Archival Cl^{-} measurements in surface water and groundwater	Data on Cl^{-}, measured monthly in the Dunajec River from 10.2022 to 10.2023 and three times (09.2022, 03.2023, and 09.2023) in four production wells (S31, S36, S37, and S39).	Personal communication with Tarnów Waterworks employee (2024)
Water production volume	Hourly data on water production volume (groundwater abstraction rate) at the Kępa Bogumiłowicka RBF site from 10.2022 to 10.2023. Information on mean daily drinking water production for the period 2015–2025.	
Hydrological observations	Data from water-gauging stations Zgłobice (WGS 84: 49.97439, 20.87943), Nowy Sącz (WGS 84: 49.62697, 20.68675), Gołkowice (WGS 84: 49.55046, 20.57058), and Nowy Targ-Kowaniec (WGS 84: 49.48688, 20.05364) on mean daily Dunajec River flow rate.	IMWM-NRI (2024)
Meteorological observations	Daily meteorological data from the stations No. 575 – Tarnów (WGS 84: 50.02986, 20.98394), No. 6525 – Polana Chochołowska (WGS 84: 49.23684, 19.78857), and No. 650 – Kasprowy Wierch (WGS 84: 49.23253, 19.98182).	

Table S3. Results of analysed $\delta^{18}O$, $\delta^{2}H$, deuterium excess (d) and Cl^- concentration in the Dunajec river and groundwater (production wells: S31, S36, S37, S39; observation well: E1), together with the Dunajec river flow rate at the sampling day.

Date	Dunajec river flow rate ($m^3 h^{-1}$)	The Dunajec River				S31				S36			
		$\delta^{18}O$ (‰)	$\delta^{2}H$ (‰)	d (‰)	Cl^- (mg L^{-1})	$\delta^{18}O$ (‰)	$\delta^{2}H$ (‰)	d (‰)	Cl^- (mg L^{-1})	$\delta^{18}O$ (‰)	$\delta^{2}H$ (‰)	d (‰)	Cl^- (mg L^{-1})
20.10.2022	44.3	-9.64	-68.1	9.0	n.m.	-9.52	-68.7	7.4	n.m.	-9.54	-68.9	7.4	n.m.
17.11.2022	24.5	-9.77	-68.7	9.4	n.m.	-9.52	-69.2	7.0	n.m.	-9.63	-69.2	7.8	n.m.
16.12.2022	43.9	-9.62	-72.1	4.9	n.m.	-9.61	-69.7	7.2	n.m.	-9.82	-68.0	10.5	n.m.
24.01.2023	99.3	-10.55	-74.0	10.4	15.3	-10.49	-73.2	10.7	15.9	-10.52	-72.2	12.0	15.9
22.02.2023	375.0	-10.92	-75.7	11.7	18.0	-11.04	-75.5	12.9	19.0	-10.86	-74.7	12.2	17.3
21.03.2023	75.2	-10.76	-74.2	11.9	14.4	-10.90	-76.0	11.2	14.7	-10.88	-75.6	11.4	15.1
28.04.2023	122.1	-10.70	-76.0	9.6	13.4	-10.60	-75.9	8.9	14.4	-10.60	-75.8	9.0	25.6
29.05.2023	79.88	-10.30	-73.4	9.0	13.5	-10.40	-73.5	9.7	14.4	-10.40	-73.8	9.4	14.9
26.06.2023	166.0	-10.50	-74.2	9.8	12.2	-10.60	-74.5	10.3	13.2	-10.60	-74.2	10.6	11.7
26.07.2023	92.9	-9.50	-66.3	9.7	13.0	-10.20	-70.6	11.0	13.1	-10.40	-71.0	12.2	12.1
06.09.2023	40.3	-9.70	-64.1	13.5	13.3	-10.00	-65.9	14.1	12.2	-9.90	-66.5	12.7	10.4
03.10.2023	53.2	-9.80	-65.8	12.6	13.8	-9.70	-64.9	12.7	13.9	-9.80	-65.1	13.3	12.1

Date	Dunajec river flow rate ($m^3 h^{-1}$)	S37				S39				E1			
		$\delta^{18}O$ (‰)	$\delta^{2}H$ (‰)	d (‰)	Cl^- (mg L^{-1})	$\delta^{18}O$ (‰)	$\delta^{2}H$ (‰)	d (‰)	Cl^- (mg L^{-1})	$\delta^{18}O$ (‰)	$\delta^{2}H$ (‰)	d (‰)	Cl^- (mg L^{-1})
20.10.2022	44.3	-9.42	-68.5	6.9	n.m.	-9.35	-69.2	5.6	n.m.	-9.29	-66.2	8.1	n.m.
17.11.2022	24.5	-9.34	-69.2	5.5	n.m.	-9.40	-69.6	5.7	n.m.	-8.97	-66.9	4.9	n.m.
16.12.2022	43.9	-9.30	-69.0	5.4	n.m.	-9.48	-67.1	8.7	n.m.	-9.04	-67.0	5.4	n.m.
24.01.2023	99.3	-9.82	-68.4	10.2	26.4	-10.01	-69.1	11.0	18.6	-9.29	-65.1	9.2	63.1
22.02.2023	375.0	-10.00	-69.4	10.6	23.6	-10.33	-71.2	11.5	15.4	-9.55	-66.7	9.8	92.0
21.03.2023	75.2	-9.60	-67.8	9.0	28.4	-9.87	-69.4	9.6	23.2	-9.38	-66.6	8.4	115.0
28.04.2023	122.1	-9.40	-67.5	7.7	31.9	-10.00	-71.9	8.1	22.7	-9.40	-67.5	7.7	93.1
29.05.2023	79.88	-9.60	-67.8	9.0	29.8	-9.90	-69.8	9.4	26.5	-9.50	-67.1	8.9	71.0
26.06.2023	166.0	-9.70	-68.4	9.2	28.9	-9.80	-69.1	9.3	28.2	-9.50	-66.7	9.3	72.7
26.07.2023	92.9	-9.90	-68.7	10.5	29.1	-10.30	-70.4	12.0	32.8	-9.90	-67.1	12.1	68.2
06.09.2023	40.3	-10.10	-68.4	12.4	27.3	-10.20	-69.6	12.0	24.1	-9.90	-66.6	12.6	63.9
03.10.2023	53.2	-10.10	-68.7	12.1	26.7	-10.10	-68.6	12.2	19.8	-9.80	-65.4	13.0	66.8

Measurement uncertainty: ±0.14‰ and ±0.66‰ for $\delta^{18}O$ and $\delta^{2}H$, respectively; n.m. – not measured; Dunajec river flow rate measured at the Zgłobice water-gauging station (Fig. 2).

Table S4. Descriptive statistics for analysed δ¹⁸O, δ²H, deuterium excess (d) and Cl⁻ concentration in the Dunajec river and groundwater (production wells: S31, S36, S37, S39; observation well: E1).

	The Dunajec				S31				S36			
	$\delta^{18}O$ (‰)	**$\delta^{2}H$** (‰)	**d** (‰)	**Cl^-** (mg L^{-1})	**$\delta^{18}O$** (‰)	**$\delta^{2}H$** (‰)	**d** (‰)	**Cl^-** (mg L^{-1})	**$\delta^{18}O$** (‰)	**$\delta^{2}H$** (‰)	**d** (‰)	**Cl^-** (mg L^{-1})
N	12	12	12	20	12	12	12	12	12	12	12	12
Mean	-10.15	-71.1	10.1	13.6	-10.21	-71.5	10.3	14.5	-10.25	-71.3	10.7	14.8
SD	0.52	4.2	2.2	1.8	0.54	3.9	2.3	1.9	0.48	3.7	2.0	4
Min	-10.92	-76.0	4.9	10	-11.04	-76.0	7.0	12	-10.88	-75.8	7.4	10.4
Q1	-10.58	-74.2	9.3	13	-10.6	-74.7	8.5	13.1	-10.6	-74.3	9.3	12.1
Q2	-10.05	-72.7	9.8	13.6	-10.3	-71.9	10.5	14.4	-10.4	-71.6	11.0	14.9
Q3	-9.68	-67.7	11.7	14.1	-9.68	-69.0	11.6	15.2	-9.82	-68.7	12.2	15.9
Max	-9.5	-64.1	13.5	18	-9.52	-64.9	14.1	19	-9.54	-65.1	13.3	25.6
Range	1.42	11.9	8.6	8	1.53	11.1	7.1	7	1.34	10.7	5.9	15.2
SE	0.15	1.2	0.6	0.4	0.16	1.1	0.7	0.6	0.14	1.1	0.6	1.2
	S37				**S39**				**E1**			
	$\delta^{18}O$ (‰)	**$\delta^{2}H$** (‰)	**d** (‰)	**Cl^-** (mg L^{-1})	**$\delta^{18}O$** (‰)	**$\delta^{2}H$** (‰)	**d** (‰)	**Cl^-** (mg L^{-1})	**$\delta^{18}O$** (‰)	**$\delta^{2}H$** (‰)	**d** (‰)	**Cl^-** (mg L^{-1})
N	12	12	12	12	12	12	12	12	12	12	12	9
Mean	-9.69	-68.5	9.0	27.8	-9.89	-69.6	9.6	22.4	-9.46	-66.6	9.1	78.4
SD	0.29	0.6	2.3	2.1	0.34	1.2	2.3	4.9	0.3	0.7	2.6	17.7
Min	-10.1	-69.4	5.4	23.6	-10.33	-71.9	5.6	15.4	-9.9	-67.5	4.9	63.1
Q1	-9.92	-68.8	7.5	26.6	-10.12	-70.0	8.6	18.9	-9.61	-67.0	8.0	66.8
Q2	-9.65	-68.4	9.1	28	-9.95	-69.5	9.5	21.9	-9.45	-66.7	9.1	71.0
Q3	-9.42	-68.3	10.5	28.9	-9.72	-69.1	11.6	24.7	-9.29	-66.5	10.4	92.0
Max	-9.3	-67.5	12.4	31.9	-9.35	-67.1	12.2	32.8	-8.97	-65.1	13.0	115.0
Range	0.8	1.9	7.0	8.3	0.98	4.8	6.6	17.4	0.93	2.4	8.1	52.0
SE	0.08	0.2	0.7	0.6	0.1	0.4	0.7	1.4	0.09	0.2	0.7	5.9

N – number of samples; SD – standard deviation; Q1 – first quartile or 25th percentile; Q2 – Second quartile or median; Q3 – Third quartile or 75th percentile; SE – standard error of the mean; Min – Minimum; Max – Maximum; Range: Max - Min.

Table S5. Descriptive statistics for water level, temperature (T), and specific conductance (SC) datalogger records in the Dunajec river and groundwater (production wells: S31, S36, S37, S39; observation well: E1).

	The Dunajec			S31			S36		
	Level (m asl)	T (°C)	SC (µS cm^{-1})	Level (m asl)	T (°C)	SC (µS cm^{-1})	Level (m asl)	T (°C)	SC (µS cm^{-1})
N	8819	8819	8161	7667	7667	7667	8819	8819	8819
Mean	189	11.64	344.9	187.15	10.8	389.7	185.71	11.1	404.7
SD	0.41	7.17	26.5	0.32	4.4	16.2	0.44	4.4	12.1
Min	188.47	0.0	254.9	186.68	3.9	351.5	184.83	5.2	308.2
Q1	188.77	4.2	324.6	186.93	7.0	379.9	185.40	6.7	398.0
Q2	188.97	11.6	336.5	187.11	9.5	386.1	185.70	10.4	405.7
Q3	189.17	19.1	368.5	187.29	14.3	394.9	185.90	15.6	414.5
Max	191.27	25.9	415.9	188.91	19.2	528.6	188.00	18.6	442.4
Range	2.8	25.9	161.0	2.23	15.4	177.1	3.17	13.3	134.2
SE	0.00	0.08	0.3	0.00	0.1	0.2	0.00	0.1	0.1
	S37			**S39**			**E1**		
	Level (m asl)	**T** (°C)	**SC** (µS cm^{-1})	**Level** (m asl)	**T** (°C)	**SC** (µS cm^{-1})	**Level** (m asl)	**T** (°C)	**SC** (µS cm^{-1})
N	8819	8819	8819	7667	7667	7667	1176	1176	1176
Mean	185.70	9.9	654.4	186.89	10.4	790.8	187.76	11.9	1089.2
SD	0.46	0.8	91.4	0.40	1.4	75.0	0.09	0.8	76.7
Min	184.78	8.5	431.0	185.93	5.1	319.3	187.60	11.0	1004.5
Q1	185.34	9.1	594.7	186.61	9.3	771.6	187.69	11.2	1037.5
Q2	185.73	10.0	656.7	187.03	10.2	805.0	187.76	11.5	1061.1
Q3	185.95	10.7	721.2	187.13	11.5	843.8	187.81	12.4	1089.5
Max	188.10	13.1	851.6	187.74	16.2	919.1	188.00	13.8	1300.5
Range	3.32	4.5	420.6	1.81	11.1	599.8	0.40	2.8	296.0
SE	0.00	0.0	1.0	0.00	0.0	0.9	0.00	0.0	2.2

Interval and frequency of the measurements: The Dunajec: water level and T: 01.10.2022–03.10.2023, hourly; SC: 01.10.2022–06.09.2023, hourly; S36 and S37: 01.10.2022–03.10.2023, hourly; S31 and S39: 18.11.2022–03.10.2023, hourly; E1: 21.03.2023–03.10.2023, every four hours. For abbreviations: see Table S4.

Table S6. Archival Cl^- concentration results in the Dunajec river and groundwater (production wells: S31, S36, S37, S39), together with the Dunajec river flow rate at the sampling day.

Date	Dunajec flow rate	Dunajec	S31	S36	S37	S39
	m^3 h^{-1}	mg L^{-1}				
14.09.2022	24.9	n.m.	16	15	28	21
03.10.2022	66.8	14	n.m.	n.m.	n.m.	n.m.
07.11.2022	22.34	14	n.m.	n.m.	n.m.	n.m.
05.12.2022	23.54	14	n.m.	n.m.	n.m.	n.m.
16.01.2023	109.2	16	n.m.	n.m.	n.m.	n.m.
20.02.2023	454.62	15	n.m.	n.m.	n.m.	n.m.
07.03.2023	80.98	n.m.	15	16	26	19
14.03.2023	104.24	13	n.m.	n.m.	n.m.	n.m.
09.05.2023	89.63	11	n.m.	n.m.	n.m.	n.m.
12.06.2023	87.27	11	n.m.	n.m.	n.m.	n.m.
04.07.2023	55.03	10	n.m.	n.m.	n.m.	n.m.
11.09.2023	35.05	14	n.m.	n.m.	n.m.	n.m.
18.09.2023	49.2	n.m.	12	12	28	18
02.10.2023	55.1	13	n.m.	n.m.	n.m.	n.m.

n.m. – not measured; Cl^- data obtained from Tarnów Waterworks; Dunajec river flow rate measured at the Zgłobice water-gauging station (Fig. 2).

Table S7. Statistical hyphothesis tests results.

Shapiro-Wilk test - d18O					T-test - d18O								Wilcoxon signed rank test - d18O			
location 1	location 2	W statistic	p-value	Normal?	Pair	t-value	df	p-value	CI (low)	CI (high)	Mean difference	Different?	Pair	V	p-value	Different?
DR	S31	0.875	0.075	Yes	DR - S31	0.956	11	0.360	-0.089	0.227	0.069	No				
DR	S36	0.726	0.002	No									DR - S36	47	0.229	No
DR	S37	0.928	0.356	Yes	DR - S37	-2.686	11	0.021	-0.828	-0.082	-0.455	Yes				
DR	S39	0.903	0.175	Yes	DR - S39	-1.658	11	0.126	-0.585	0.082	-0.251	No				
DR	E1	0.908	0.201	Yes	DR - E1	-3.785	11	0.003	-1.083	-0.287	-0.685	Yes				
S31	E1	0.937	0.462	Yes	S31 - E1	-4.710	11	0.001	-1.106	-0.401	-0.754	Yes				
S36	E1	0.935	0.432	Yes	S36 - E1	-5.317	11	<0.001	-1.111	-0.460	-0.786	Yes				
S37	E1	0.965	0.853	Yes	S37 - E1	-4.858	11	0.001	-0.334	-0.126	-0.230	Yes				
S39	E1	0.952	0.667	Yes	S39 - E1	-7.677	11	<0.001	-0.558	-0.309	-0.434	Yes				

Shapiro-Wilk test - d2H					T-test - d2H								Wilcoxon signed rank test - d2H			
location 1	location 2	W statistic	p-value	Normal?	Pair	t-value	df	p-value	CI (low)	CI (high)	Mean difference	Different?	Pair	V	p-value	Different?
DR	S31	0.929	0.372	Yes	DR - S31	0.851	11	0.413	-0.651	1.472	0.411	No				
DR	S36	0.969	0.898	Yes	DR - S36	0.327	11	0.750	-1.170	1.578	0.204	No				
DR	S37	0.894	0.131	Yes	DR - S37	-2.027	11	0.068	-5.361	0.220	-2.570	No				
DR	S39	0.815	0.014	No									DR - S39	24	0.266	No
DR	E1	0.897	0.147	Yes	DR - E1	-3.785	11	0.003	-7.088	-1.876	-4.482	Yes				
S31	E1	0.890	0.118	Yes	S31 - E1	-4.619	11	0.001	-7.224	-2.561	-4.892	Yes				
S36	E1	0.892	0.124	Yes	S36 - E1	-4.706	11	0.001	-6.877	-2.494	-4.686	Yes				
S37	E1	0.966	0.867	Yes	S37 - E1	-6.686	11	<0.001	-2.541	-1.282	-1.912	Yes				
S39	E1	0.870	0.065	Yes	S39 - E1	-9.236	11	<0.001	-3.723	-2.290	-3.007	Yes				

Shapiro-Wilk test - Cl-					T-test - Chloride								Wilcoxon signed rank test - Cl-			
location 1	location 2	W statistic	p-value	Normal?	Pair	t-value	df	p-value	CI (low)	CI (high)	Mean difference	Different?	Pair	V	p-value	Different?
DR	S31	0.837	0.053	Yes	DR - S31	-1.89	8	0.096	-0.95	0.09	-0.43	No				
DR	S36	0.680	0.001	No									DR - S36	24	0.910	No
DR	S37	0.901	0.261	Yes	DR - S37	-10.85	8	<0.001	-16.86	-10.95	-13.90	Yes				
DR	S39	0.991	0.998	Yes	DR - S39	-4.19	8	0.003	-14.55	-4.23	-9.39	Yes				
DR	E1	0.858	0.092	Yes	DR - E1	-11.18	8	<0.001	-77.60	-51.06	-64.33	Yes				
S31	E1	0.848	0.072	Yes	S31 - E1	-11.24	8	<0.001	-77.01	-50.80	-63.90	Yes				
S36	E1	0.826	0.041	No									S36 - E1	0	0.004	Yes
S37	E1	0.793	0.017	No									S37 - E1	0	0.004	Yes
S39	E1	0.832	0.047	No									S39 - E1	0	0.004	Yes

Shapiro-Wilk test - SC					Wilcoxon signed rank test - SC			
location 1	location 2	W statistic	p-value	Normal?	Pair	V	p-value	Different?
DR	S31	0.822	<0.001	No	DR - S31	0	<0.001	Yes
DR	S36	0.976	0.005	No	DR - S36	0	<0.001	Yes
DR	S37	0.963	<0.001	No	DR - S37	0	<0.001	Yes
DR	S39	0.866	<0.001	No	DR - S39	0	<0.001	Yes
DR	E1	0.802	<0.001	No	DR - E1	0	<0.001	Yes
S31	E1	0.828	<0.001	No	S31 - E1	0	<0.001	Yes
S36	E1	0.790	<0.001	No	S36 - E1	0	<0.001	Yes
S37	E1	0.931	<0.001	No	S37 - E1	0	<0.001	Yes
S39	E1	0.808	<0.001	No	S39 - E1	0	<0.001	Yes

DR – Dunajec River, S31, S36, S37, S39 – production wells, E1– observation well

Table S8. Fraction (f) of the end-members (i) Dunajec River water and (ii) native groundwater in the groundwater of the production wells S31, S36, S37 and S39.

End-member	$\delta^{18}O$ during the entire sampling period (October 2022–October 2023)											
	S31			S36			S37			S39		
	f	SE	p-value	f	SE	p-value	f	SE	p-value	f	SE	p-value
The Dunajec	0.98	0.08	<0.001	0.97	0.09	<0.001	0.23	0.06	0.002	0.44	0.08	<0.001
Native groundwater	0.03	0.08	0.383	0.03	0.09	0.369	0.77	0.06	<0.001	0.56	0.08	<0.001

End-member	$\delta^{18}O$ from January 2023 to June 2023 (high meltwater contribution)											
	S31			S36			S37			S39		
	f	SE	p-value	f	SE	p-value	f	SE	p-value	f	SE	p-value
The Dunajec	1.04	0.04	<0.001	1.01	0.03	<0.001	0.21	0.07	0.015	0.46	0.05	<0.001
Native groundwater	-0.04	0.04	0.165	-0.01	0.03	0.360	0.79	0.07	<0.001	0.54	0.05	<0.001

End-member	$\delta^{18}O$ with the memory effect considered											
	S31			S36			S37			S39		
	f	SE	p-value	f	SE	p-value	f	SE	p-value	f	SE	p-value
The Dunajec	1.08	0.11	<0.001	1.12	0.15	<0.001	0.23	0.09	0.013	0.47	0.14	0.004
Native groundwater	-0.08	0.11	0.258	-0.12	0.15	0.227	0.77	0.09	<0.001	0.53	0.14	0.002
Memory effect	0.38	0.12	0.008	0.51	0.13	0.002	0.25	0.29	0.212	0.37	0.31	0.133

End-member	$\delta^{2}H$ during the entire sampling period (October 2022–October 2023)											
	S31			S36			S37			S39		
	f	SE	p-value	f	SE	p-value	f	SE	p-value	f	SE	p-value
The Dunajec	0.97	0.08	<0.001	0.90	0.10	<0.001	0.22	0.09	0.013	0.40	0.11	0.002
Native groundwater	0.03	0.08	0.374	0.10	0.10	0.177	0.78	0.09	<0.001	0.60	0.11	<0.001

End-member	$\delta^{2}H$ from January 2023 to June 2023 (high meltwater contribution)											
	S31			S36			S37			S39		
	f	SE	p-value	f	SE	p-value	f	SE	p-value	f	SE	p-value
The Dunajec	1.02	0.04	<0.001	0.97	0.06	<0.001	0.21	0.06	0.012	0.44	0.03	<0.001
Native groundwater	-0.02	0.04	0.353	0.04	0.06	0.281	0.79	0.06	<0.001	0.56	0.03	<0.001

End-member	$\delta^{2}H$ with the memory effect considered											
	S31			S36			S37			S39		
	f	SE	p-value	f	SE	p-value	f	SE	p-value	f	SE	p-value
The Dunajec	1.08	0.09	<0.001	1.04	0.13	<0.001	0.11	0.51	0.414	0.45	0.22	0.039
Native groundwater	-0.08	0.09	0.183	-0.04	0.13	0.373	0.89	0.51	0.059	0.55	0.22	0.020
Memory effect	0.42	0.08	<0.001	0.48	0.10	0.001	0.92	0.14	<0.001	0.64	0.21	0.008

End-member	Cl^- from January 2023 to October 2023											
	S31			S36			S37			S39		
	f	SE	p-value	f	SE	p-value	f	SE	p-value	f	SE	p-value
The Dunajec	0.99	0.00	<0.001	0.98	0.02	<0.001	0.80	0.03	<0.001	0.87	0.04	<0.001
Native groundwater	0.01	0.00	0.034	0.02	0.02	0.193	0.20	0.03	<0.001	0.13	0.04	0.005

End-member	Cl^- without the months with elevated native groundwater Cl^- content (February, March, and April 2023)											
	S31			S36			S37			S39		
	f	SE	p-value	f	SE	p-value	f	SE	p-value	f	SE	p-value
The Dunajec	0.99	0.01	<0.001	1.01	0.01	<0.001	0.73	0.01	<0.001	0.78	0.04	<0.001
Native groundwater	0.01	0.01	0.200	-0.01	0.01	0.191	0.27	0.01	<0.001	0.22	0.04	0.003

End-member	Cl^- with the memory effect considered											
	S31			S36			S37			S39		
	f	SE	p-value	f	SE	p-value	f	SE	p-value	f	SE	p-value
The Dunajec	0.99	0.00	<0.001	0.98	0.03	<0.001	0.77	0.06	<0.001	0.83	0.11	<0.001
Native groundwater	0.01	0.00	0.079	0.02	0.03	0.277	0.23	0.06	0.007	0.17	0.11	0.093
Memory effect	0.01	0.14	0.467	0.20	0.38	0.308	0.78	0.14	0.001	0.74	0.23	0.012

End-member	SC (daily resolution from 22.03.2023 to 06.09.2023)											
	S31			S36			S37			S39		
	f	SE	p-value	f	SE	p-value	f	SE	p-value	f	SE	p-value
The Dunajec	0.92	0.01	<0.001	0.94	0.09	<0.001	0.54	0.07	<0.001	0.37	0.03	<0.001
Native groundwater	0.08	0.01	<0.001	0.06	0.09	<0.001	0.46	0.07	<0.001	0.63	0.03	<0.001
Memory effect	0.92	0.03	<0.001	1.00	0.01	<0.001	0.96	0.02	<0.001	0.88	0.04	<0.001

f - The estimated fraction of an end-member in the mixed water; SE – Standard error; p-value – When the p-value is less than 0.05, the result can be considered statistically significant. The p-values are one-tailed (Kirchner, 2023).

Table S9. Fraction (f) of the end-members (i) Dunajec river water and (ii) native groundwater in the groundwater of the production wells S31, S36, S37 and S39 during the months with no meltwater contribution.

End-member	$\delta^{18}O$ from October 2022 to December 2022 (no meltflow contribution)											
	S31			S36			S37			S39		
	f	SE	p-value	f	SE	p-value	f	SE	p-value	f	SE	p-value
The Dunajec River	0.77	0.10	0.04	0.97	0.18	0.06	0.45	0.02	0.01	0.57	0.12	0.07
Native groundwater	0.23	0.10	0.13	0.03	0.18	0.45	0.55	0.02	0.01	0.44	0.12	0.09
End-member	**$\delta^{18}O$ from July 2023 to October 2023 (no meltflow contribution)**											
	S31			**S36**			**S37**			**S39**		
	f	SE	p-value	f	SE	p-value	f	SE	p-value	f	SE	p-value
The Dunajec River	-0.70	0.17	0.08	-1.00	0.35	0.11	-0.20	0.55	0.39	-1.10	0.50	0.14
Native groundwater	1.70	0.17	0.03	2.00	0.35	0.06	1.20	0.55	0.14	2.10	0.50	0.07
End-member	**$\delta^{2}H$ from October 2022 to December 2022 (no meltflow contribution)**											
	S31			**S36**			**S37**			**S39**		
	f	SE	p-value	f	SE	p-value	f	SE	p-value	f	SE	p-value
The Dunajec River	0.69	0.21	0.10	0.46	0.33	0.20	0.58	0.23	0.12	0.35	0.43	0.28
Native groundwater	0.31	0.21	0.19	0.54	0.33	0.17	0.42	0.23	0.16	0.65	0.43	0.18
End-member	**$\delta^{2}H$ from July 2023 to October 2023 (no meltflow contribution)**											
	S31			**S36**			**S37**			**S39**		
	f	SE	p-value	f	SE	p-value	f	SE	p-value	f	SE	p-value
The Dunajec River	-0.18	0.95	0.44	-0.42	1.00	0.37	-0.63	0.99	0.32	-1.26	1.16	0.24
Native groundwater	1.18	0.95	0.22	1.42	1.00	0.20	1.63	0.99	0.17	2.26	1.16	0.15

f – Estimated fraction of the end-member in the mixed water; SE – Standard error; p-value – When the p-value is less than 0.05, the result can be considered statistically significant. The p-values are one-tailed (Kirchner, 2023).

Supplementary Figures

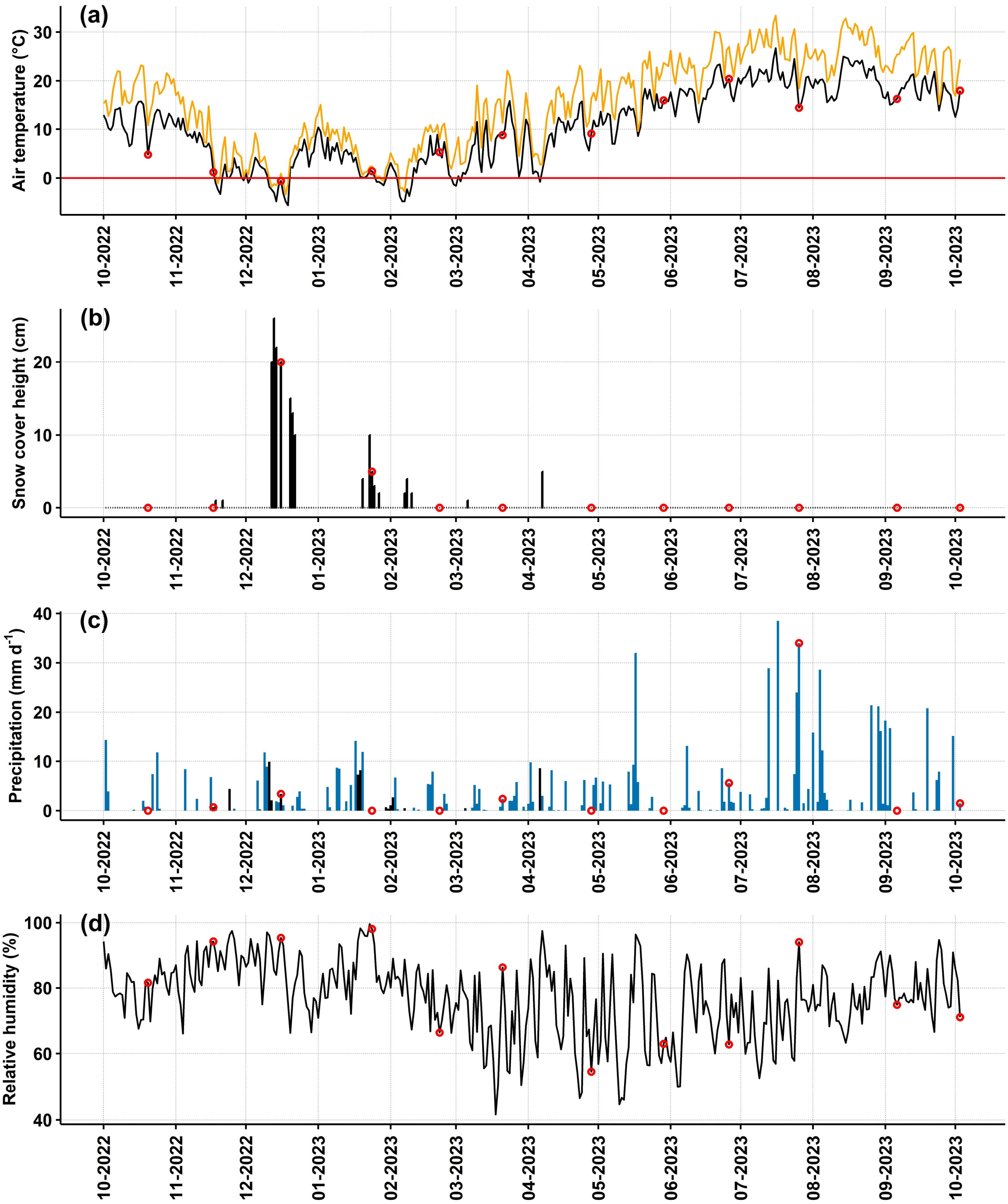

Figure S1: Mean (black) and maximum (orange) daily air temperature, red horizontal line marks temperature of 0°C (a), snow cover height (b), precipitation in the form of rain (blue) or snow (black) (c), and relative air humidity (d) in Tarnów during the sampling period (October 2022–October 2023). Sampling days are marked as red circles.

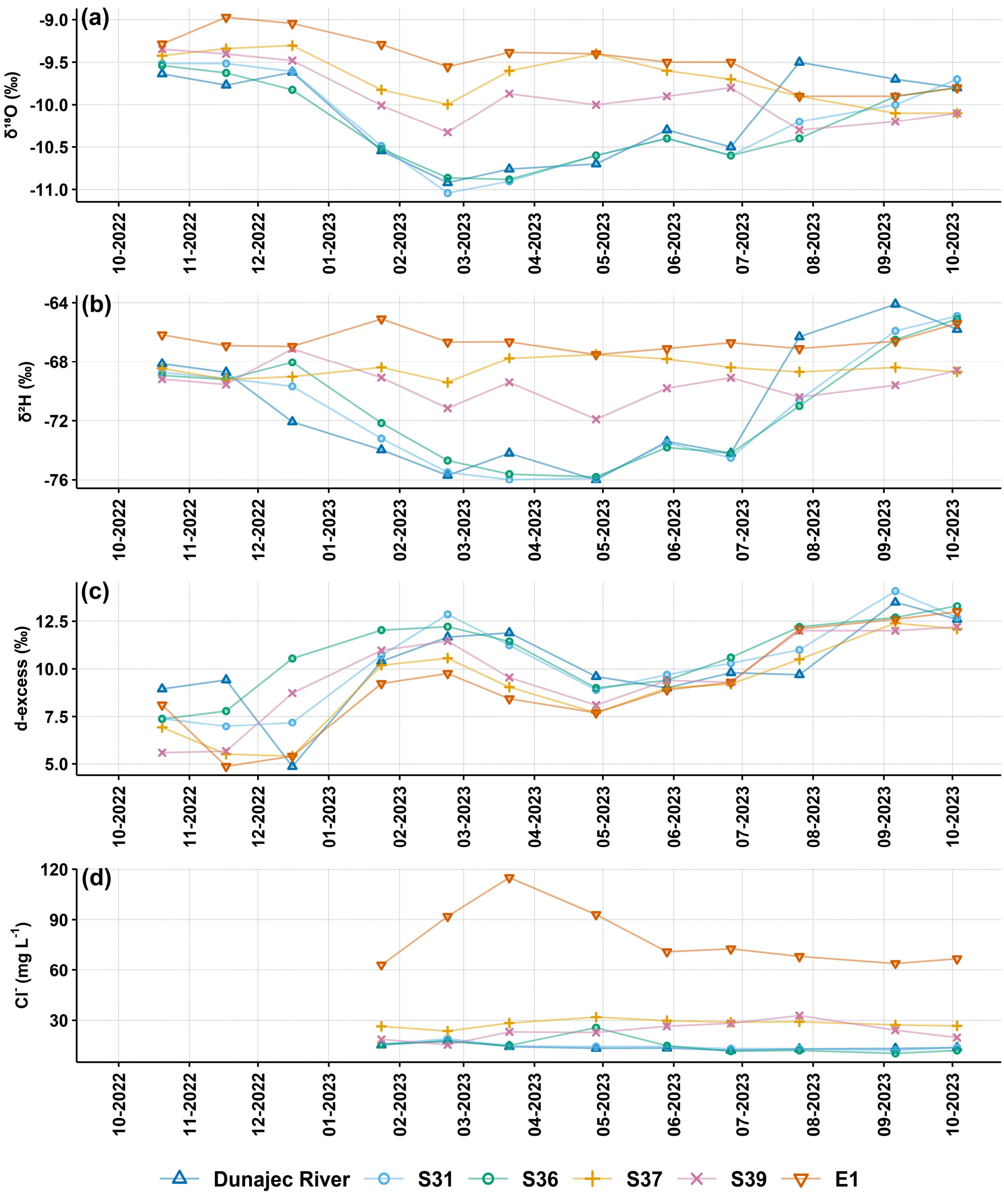

Figure S2: $\delta^{18}O$ (a), $\delta^{2}H$ (b), d-excess (c), and chloride (d) in the Dunajec river water and groundwater in the study area throughout the sampling period.

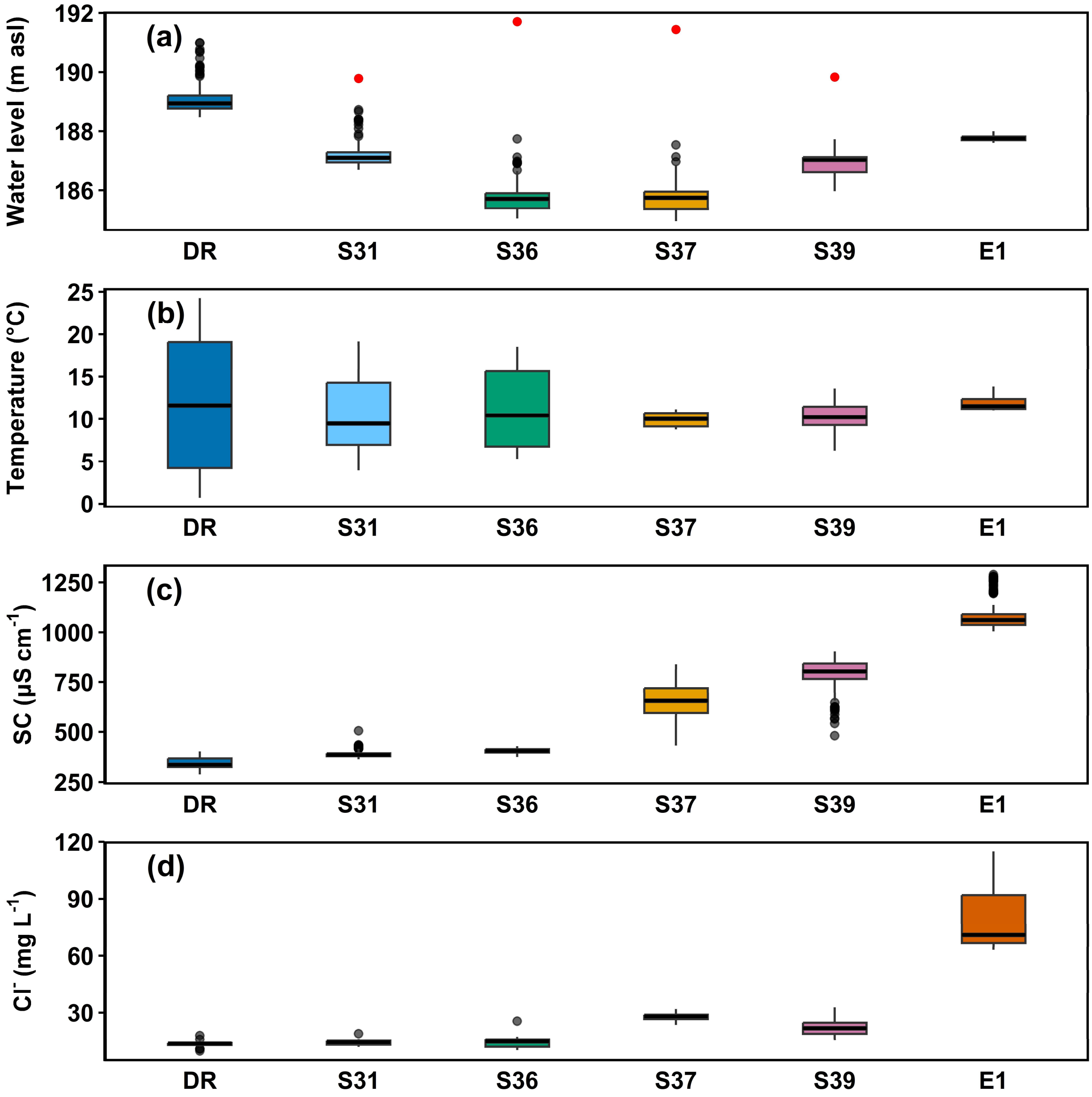

Figure S3: Box plots of measured daily water level (a), temperature - T (b), specific conductance - SC (c), and chloride concentration – Cl^- (d) in the Dunajec River (DR), four RBF site wells (S31, S36, S37, S39), and the E1 observation well during the sampling period (October 2022–October 2023). Boxes extend from the first quartile (Q1) to the third quartile (Q3); black horizontal lines within the boxes show the medians. The whiskers extend from the box to values ±1.5 × the inter-quartile range (IQR). Grey dots outside the whiskers mark outliers. The red dots on plot (a) are the terrain levels for each production well. Number (n) of observations per sampling location: water level and T: DR, S36, S37: n = 368; S31, S39: n = 320; E1: n = 197; SC: DR: n = 342; S36, S37: n = 368; S31, S39: n = 320; E1: n = 197; Cl^- in DR: n = 20; Cl^- in S31, S36, S37, S39: n = 12; Cl^- in E1: n = 9.

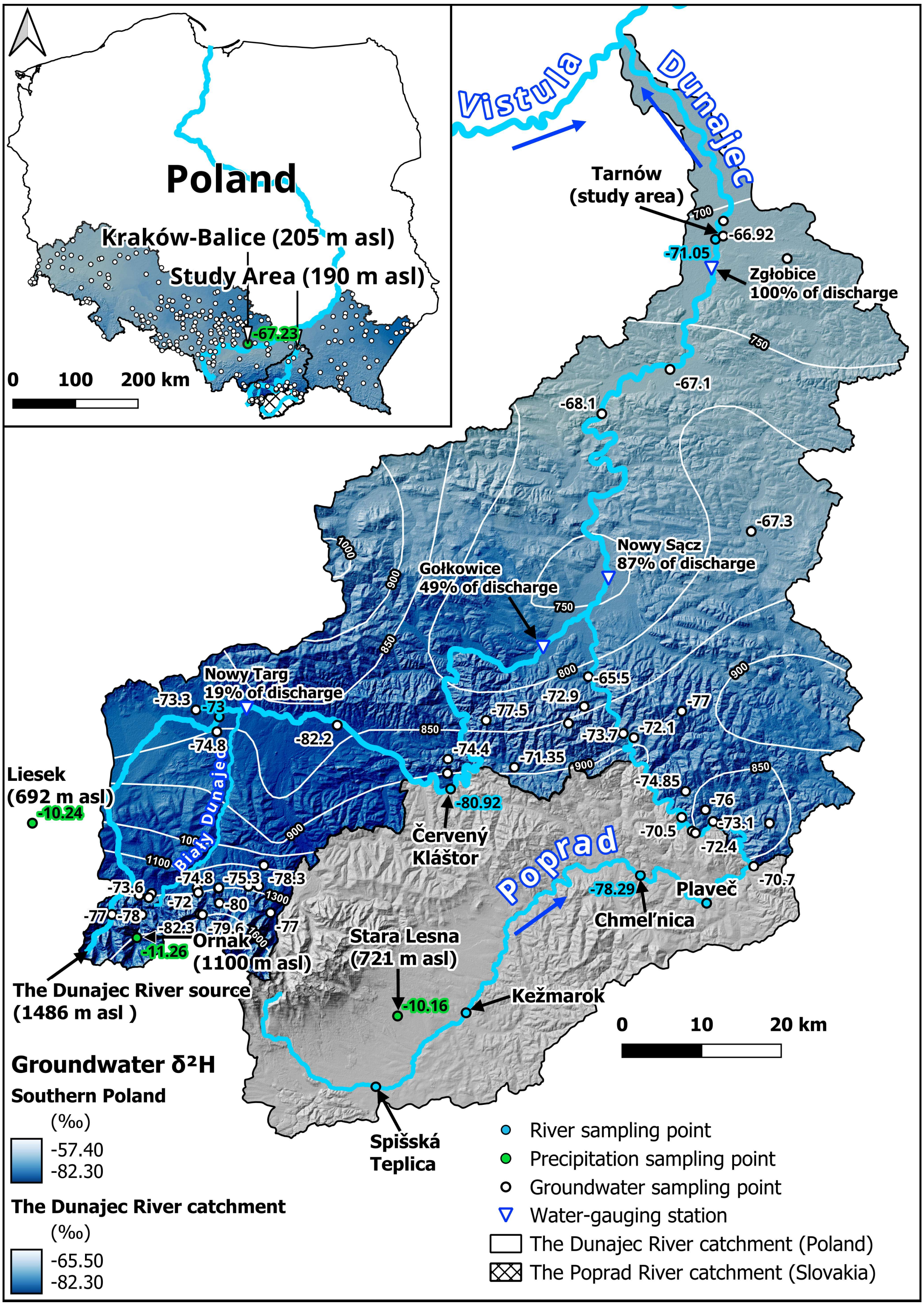

Figure S4: Distribution of δ^2H in precipitation, river water, and recent groundwater across the Dunajec catchment on the Polish and Slovak territory (constituted there by the Poprad catchment). For a broader perspective, the distribution of δ^2H in recent groundwaters in southern Poland is also shown. White isolines show the mean annual precipitation (in mm) in the Polish part of the Dunajec catchment from 1981-2010, based on Kruk et al. (2017). "% of discharge" refers to the mean Dunajec flow rate in Tarnów calculated for 2000–2022 (water-gauging station: Zgłobice). Thus, e.g., 87% in a water-gauging station upstream indicates that 87% of the Dunajec flow rate noted at Zgłobice was recorded on average from 2000–2022 at this station. Digital Elevation Model (DEM) source: NASA Shuttle Radar Topography Mission (2013).

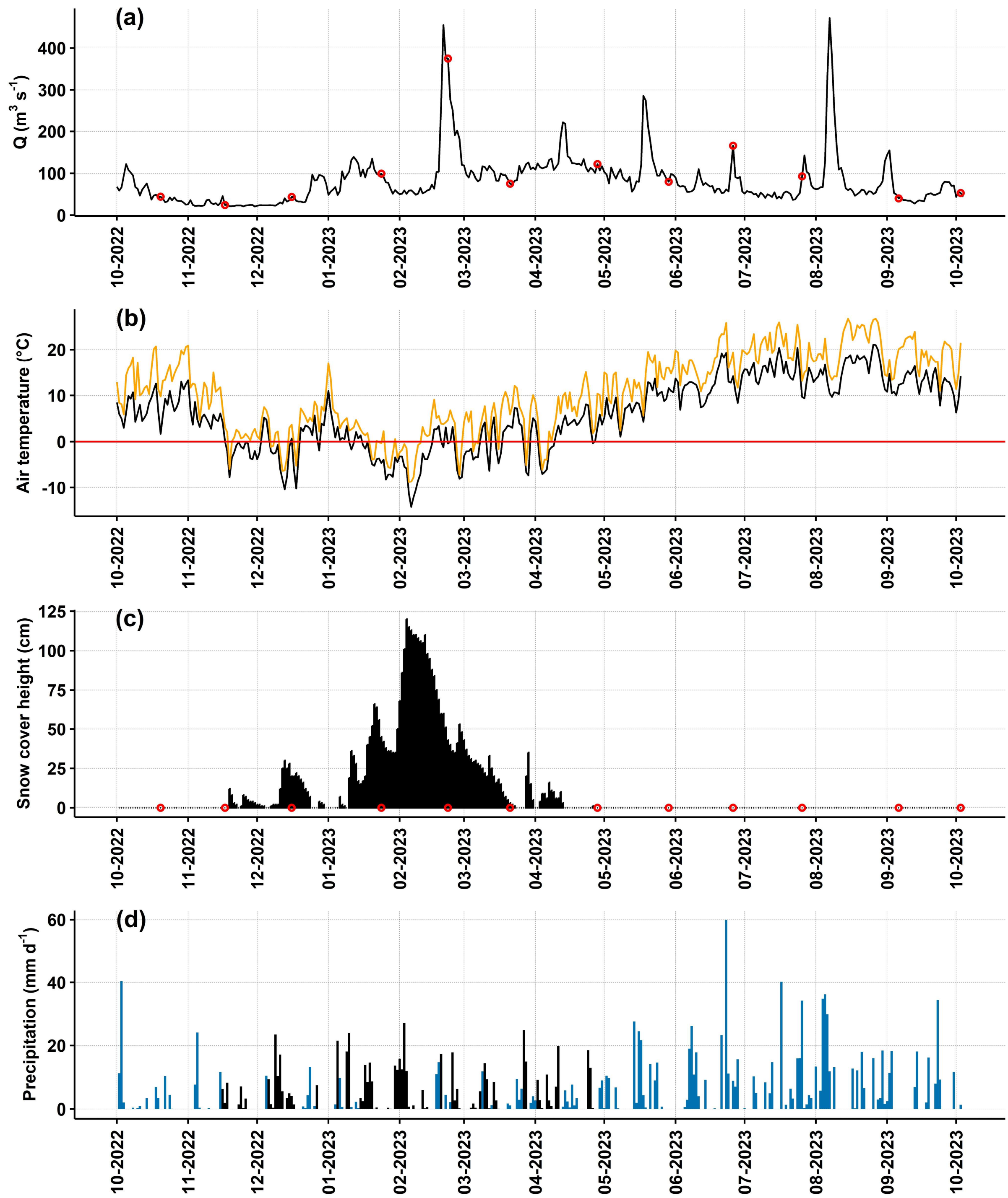

Figure S5: Mean daily flow rate of the Dunajec river recorded at the Zgłobice water-gauging station, with sampling days of this study marked as red circles (a), along with mean (black) and maximum (orange) daily air temperature with 0°C threshold marked by the red horizontal line (b), snow cover height, with sampling days of this study marked as red circles (c), and precipitation in the form of rain (blue) or snow (black) (d). Weather data on plots (b) – (d) recorded at the Polana Chochołowska station (Fig. 2) during the sampling period.

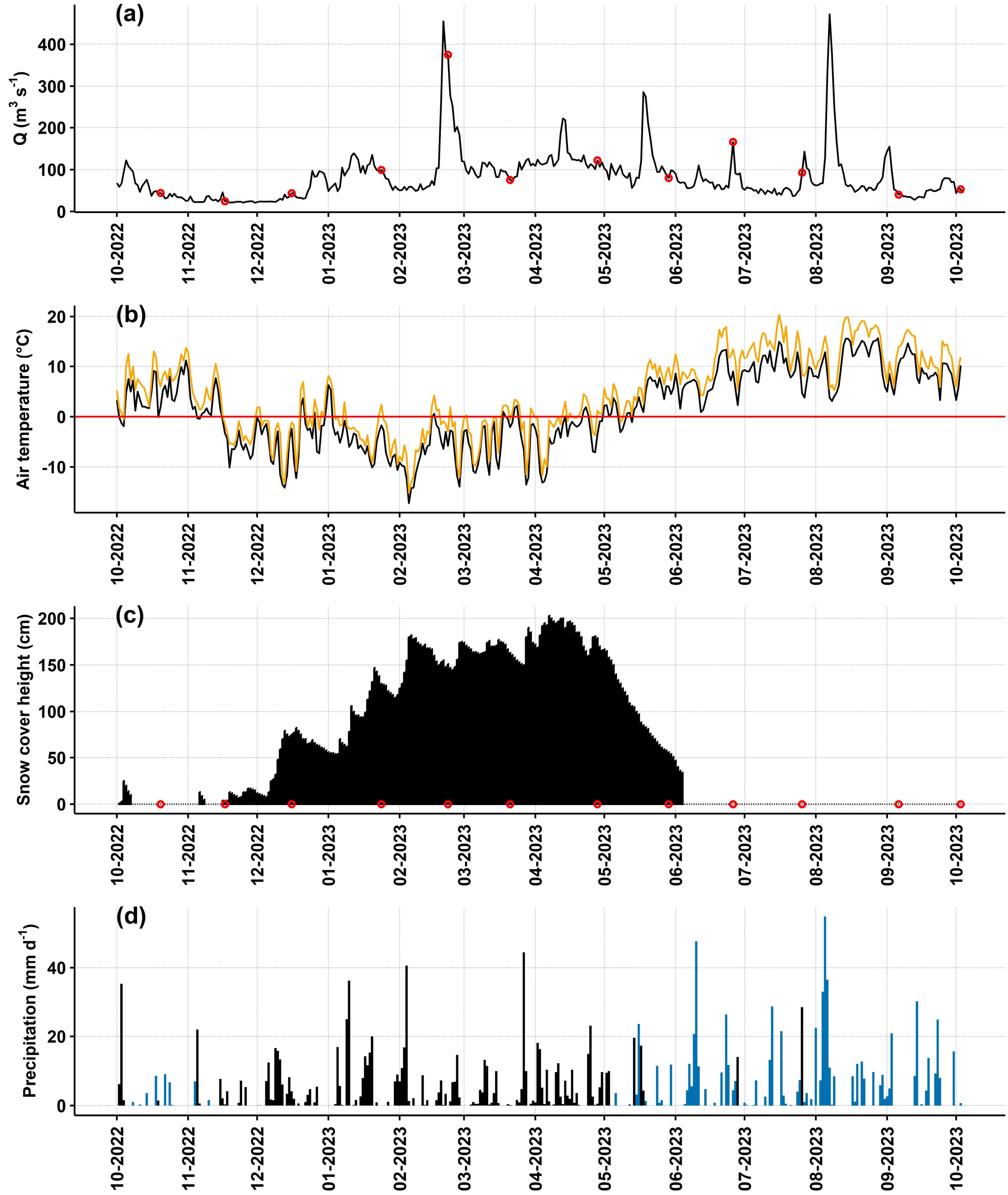

Figure S6: Mean daily flow rate of the Dunajec river recorded at the Zgłobice water-gauging station, with sampling days of this study marked as red circles (a), along with mean (black) and maximum (orange) daily air temperature with 0°C threshold marked by the red horizontal line (b), snow cover height, with sampling days of this study marked as red circles (c), and precipitation in the form of rain (blue) or snow (black) (d). Weather data on plots (b) – (d) recorded at the Kasprowy Wierch station (Fig. 2) during the sampling period.

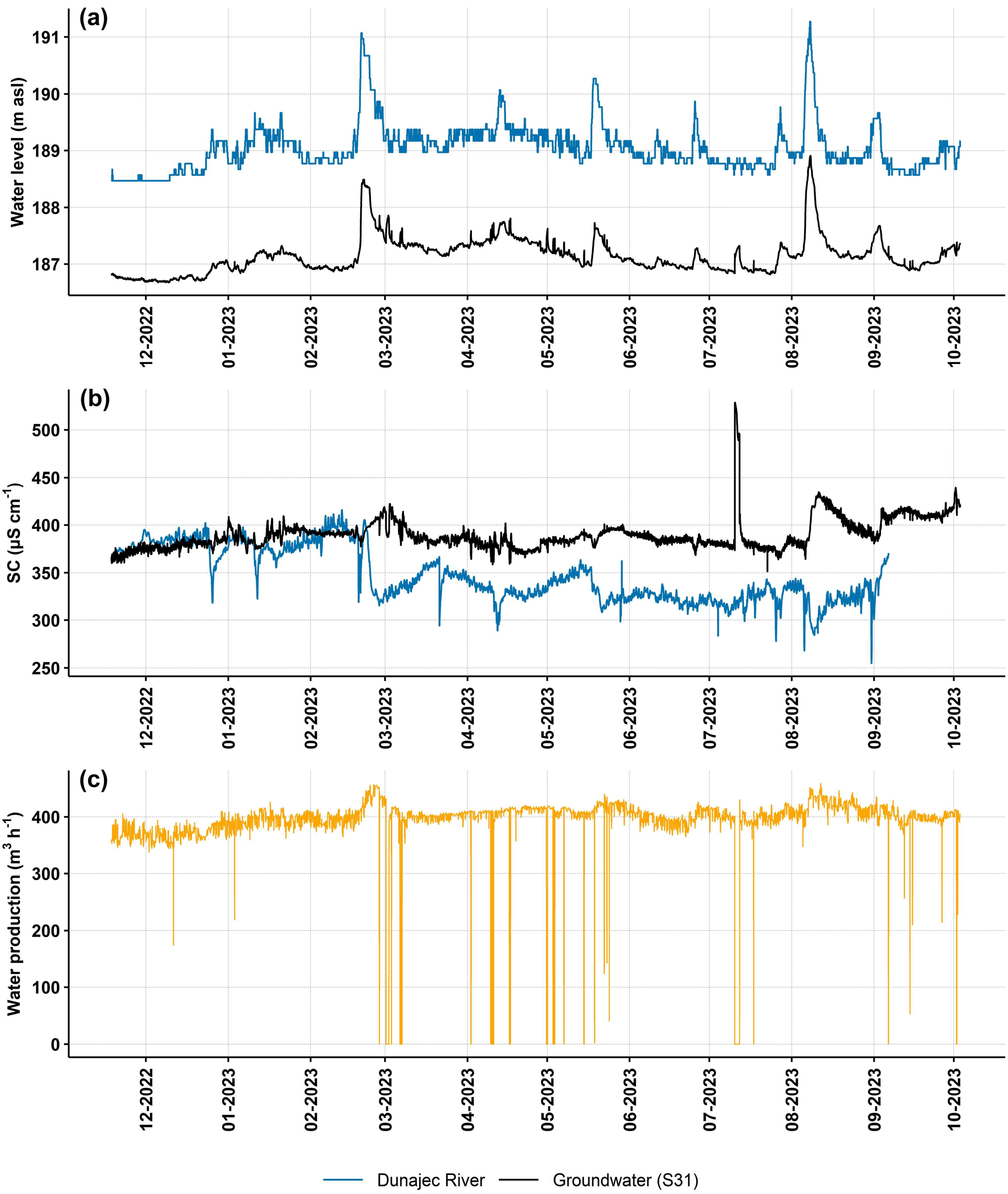

Figure S7: Hourly measurements of the Dunajec River level (recorded at the surface water intake, Fig. 1) and S31 groundwater level (a) and specific conductance (SC) recorded in the Dunajec and S31 (b), as well as hourly measurements of water production (groundwater abstraction) at the well field (c).

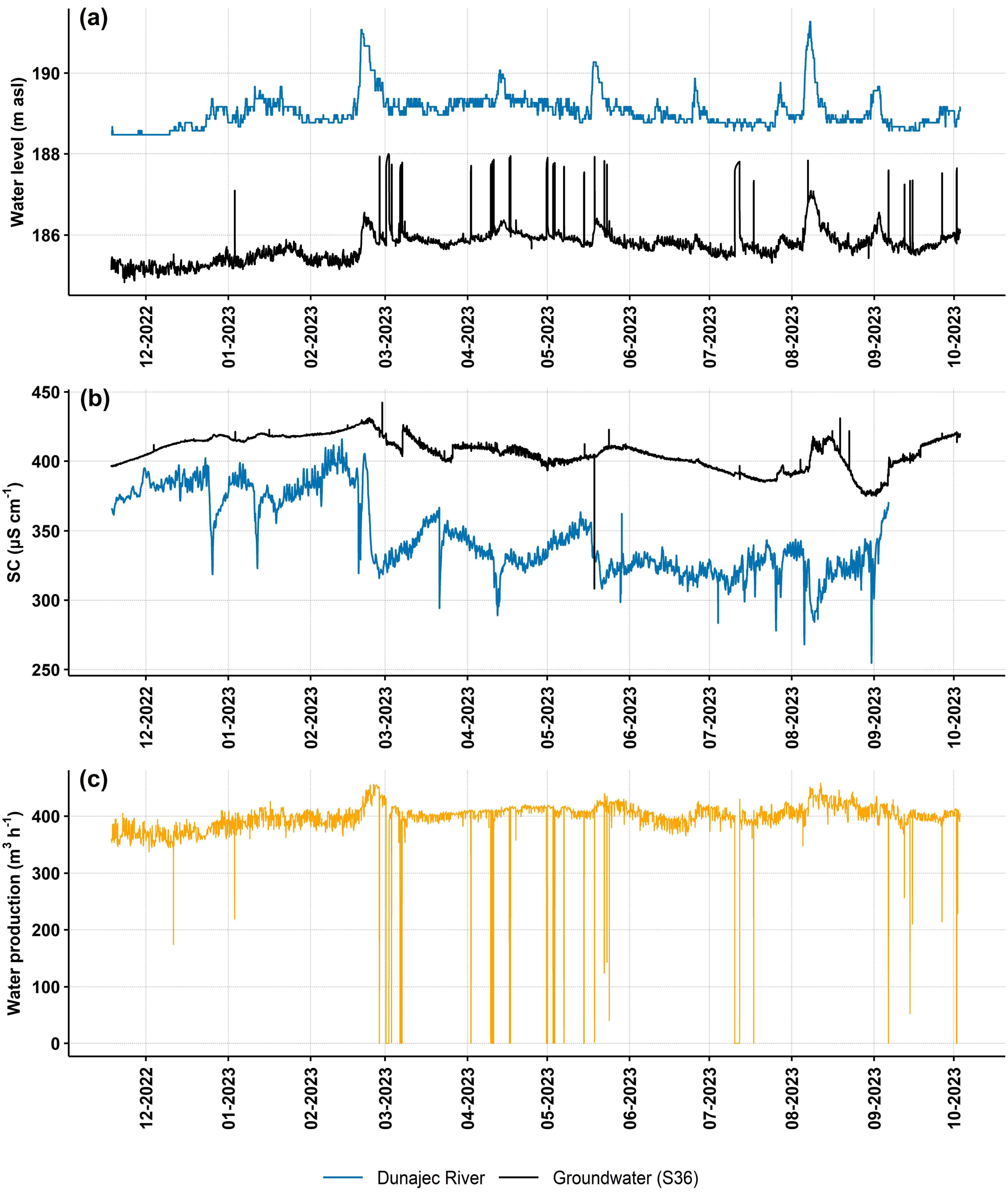

Figure S8: Hourly measurements of the Dunajec River level (recorded at the surface water intake, Fig. 1) and S36 groundwater level (a) and specific conductance (SC) recorded in the Dunajec and S36 (b), as well as hourly measurements of water production (groundwater abstraction) at the well field (c).

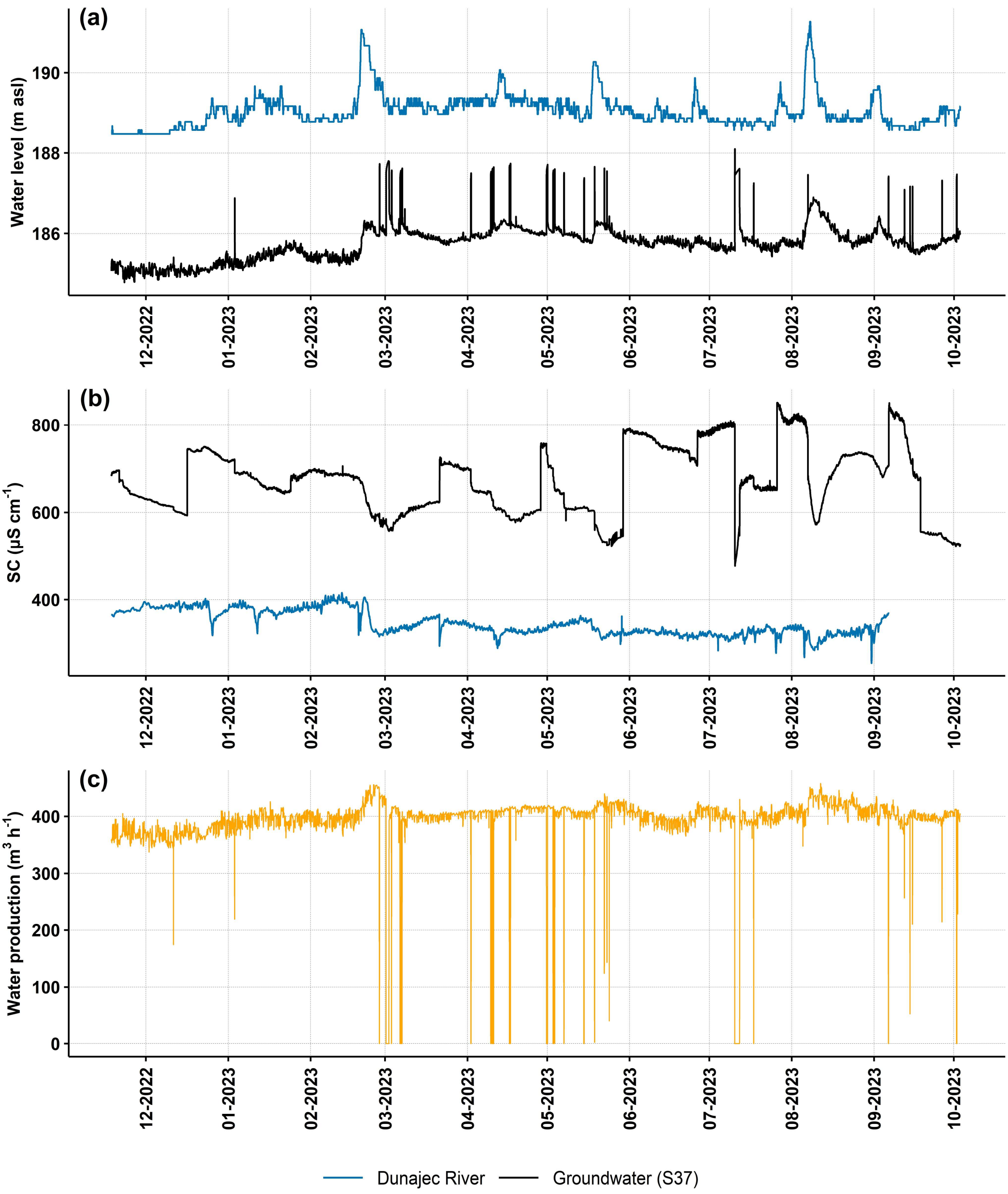

Figure S9: Hourly measurements of the Dunajec River level (recorded at the surface water intake, Fig. 1) and S37 groundwater level (a) and specific conductance (SC) recorded in the Dunajec and S37 (b), as well as hourly measurements of water production (groundwater abstraction) at the well field (c).

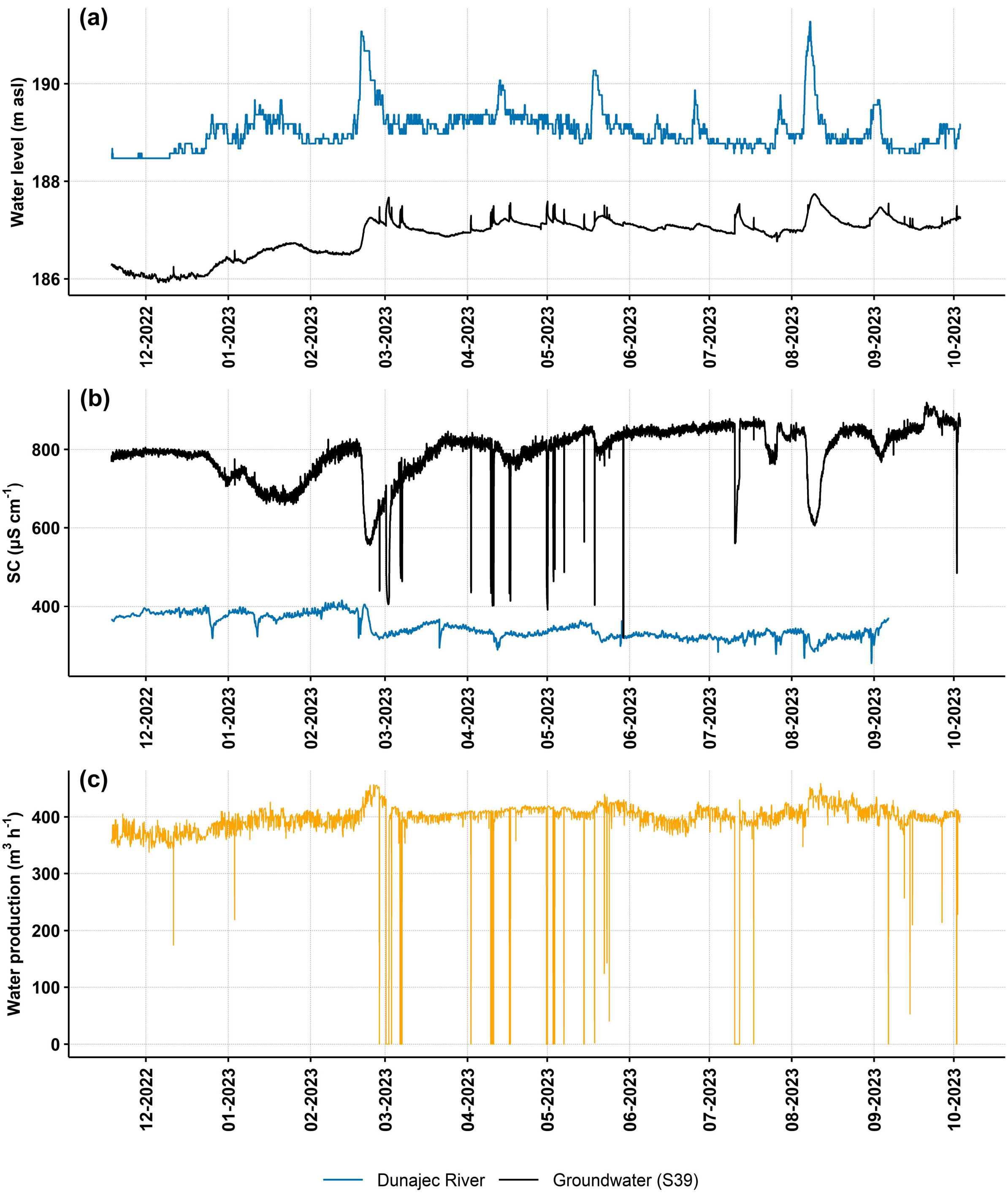

Figure S10: Hourly measurements of the Dunajec river level (recorded at the surface water intake, Fig. 1) and S39 groundwater level (a) and specific conductance (SC) recorded in the Dunajec and S39 (b), as well as hourly measurements of water production (groundwater abstraction) at the well field (c).

Sections supplementing the research

S1 Detailed interpretation of the Dunajec regime impact on abstracted water isotopic composition, divided into three intervals

As pointed out in Section 4.1, climate change increasingly alters snowmelt timing and intensity across mid-latitude regions. Notably, long-term data (1966–2021) for Tarnów show that the region exhibits a warming trend of 0.4 °C per decade (Sitek et al., 2021). Since the late 1990s, the frequency of wet days and days with precipitation ≥10 mm has decreased, while extreme rainfall events (the daily total >30 mm) have become more frequent (Sitek et al., 2021), echoing southern-Poland trends (Falarz, 2021). This shift amplifies drought- and flood-risk, increases RBF variability at the well field in the study, and may worsen as upstream reservoirs lose retention capacity (Sitek et al., 2025). In this supplementing section, we divide the observation period into three time intervals during which different sources constituted the Dunajec River flow.

S1.1 Early October 2022 to late December 2022

The $\delta^{18}O$ and $\delta^{2}H$ values of samples from production wells S31, S36, S37, and S39 collected in October and November 2022 were similar and plotted slightly below the LMWL (Fig. 5), indicating minor evaporation. Dunajec samples from the same period were located nearby on the water mixing line, showing slightly more depleted values than the most enriched E1 samples (Fig. 5). This pattern suggests a notable contribution of native groundwater (baseflow) and rainfall to the recharge of both the Dunajec and the production wells given the river's substantial role in aquifer recharge. Calculations for 1970–2022 estimate that baseflow accounts for, on average, 54% of the total Dunajec flow in the Tarnów region (Janik et al., 2024).

It should be noted that (a) approximately 87% of the Dunajec discharge recorded at the Zgłobice station is already established in the city of Nowy Sącz, 73 km upstream of the Kępa Bogumiłowicka RBF site (Fig. 7), and (b) the Poprad significantly contributes to the Dunajec flow, accounting for an average of 34% of total discharge between 2000 and 2022 (IMWM-NRI, 2024). Hence, it strongly influences its isotopic composition throughout the year (Fig. 7). Consequently, while $\delta^{18}O$ and $\delta^{2}H$ values of the Dunajec water tend to be more enriched in the northern part of the catchment due to partial evaporation during flow, they are primarily determined by recharge processes in the southern and central catchment. Native groundwater from the Tarnów region also affects these values, though to a limited extent, mainly during dry periods when Tatra meltwater is absent.

In October and November 2022, mean air temperatures in Tarnów were 11.6 °C and 4.9 °C, respectively, with relative humidity at 80.5% and 87.5%. These conditions could have favoured evaporation, as suggested also by lower d-excess values observed in those months (Fig. S2c). Given the young age and shallow circulation system of native groundwater in Tarnów, its mean isotopic composition closely resembled that of Kraków precipitation (Fig. 5), in agreement with findings from recent groundwater isoscape research in Poland (Leśniak and Wilamowski, 2019).

Compared to October and November, December 2022 samples showed more dispersion on the bivariate plot (Fig. 5), likely linked to the first and largest snowfall and snowmelt event in Tarnów during the sampling period (Fig. S1). Snow cover reached 26 cm on 13 December but dropped to 0 cm by 15 December (IMWM-NRI, 2024). The Dunajec sample from 16 December, collected after renewed snowfall, likely contained partially evaporated snowmelt entering the river via surface runoff. A similar process was described by Kalvāns et al. (2020) in the Salaca River catchment (Latvia). Due to the short time between snowmelt and sampling, this effect has not yet been reflected in the wells, whose December isotope values resembled those from November, where S37 and S39 remained closer to native groundwater, while the Dunajec influenced S31 and S36 more. At the same time, native groundwater likely contributed highly to Dunajec recharge in December, as evidenced by similar d-excess values in E1 and the river (Fig. S2c). Aside from a few days of elevated flow rate in early October due to rainfall in Tarnów and the southern catchment (Fig. S1, Fig. S5–S6), the end of 2022 was marked by low flows, averaging 38.5 $m^3 s^{-1}$ between 1 October and 22 December.

S1.2 Late December 2022 to late June 2023

Stable water isotope results indicate that January 2023 was the first month with a clear meltwater contribution to the Dunajec discharge. However, the initial snowmelt surge during the study period occurred, in fact, at the end of December 2022, one week after the sampling. Heavy snowfall was recorded in the Tatra Range in early December, and the first day with temperatures well above 0 °C at station No. 6525 (near the Dunajec source; Fig. 2) was 20 December (Fig. S5). The resulting increase in discharge at the Zgłobice station was observed three days after (Fig. S5). The final week of December was marked by elevated river flow, averaging 76.0 $m^3 s^{-1}$ (IMWM-NRI, 2024). Between late December 2022 and the end of June 2023, a sustained contribution of meltwater to the Dunajec flow was evidenced by stable water isotope and hydrological data (Fig. 4). During this period, isotope values from the river and wells S31 and S36 were closely aligned, showing depleted signatures clustered in the lower left of the dual isotope plot, with minimum $\delta^{18}O$ and $\delta^{2}H$ values reaching –10.25‰ and –72‰, respectively (Fig. 5). From 23 December to 30 June, the mean river discharge at the Zgłobice station was 105.3 $m^3 s^{-1}$, with four prominent flow peaks, primarily driven by snowmelt and rainfall. The highest daily discharge (454.6 $m^3 s^{-1}$) was recorded on 20 February, four days after a sharp rise in air temperature in the Tatras (Fig. S5). This surge was attributed to meltwater from the lower Tatras, where positive temperatures were recorded at station No. 6525 (1145 m asl), while station No. 650 (1990 m asl) continued to register sub-zero values. The higher station's mean daily temperatures did not exceed 0 °C until early May (Fig. S6). Subsequent flow increases in May and June were primarily linked to meltwater and heavy rainfall in the higher Tatras. The May peak was meltwater-dominated, while the June peak was mainly rainfall-driven. No snow cover was recorded at station No. 650 after early June (Fig. S6), though snowmelt likely persisted in the highest parts of the Tatras (approx. 2000–2600 m asl), as suggested by the continued depletion of $\delta^{18}O$ and $\delta^{2}H$ values observed at the study site in late June (Fig. S2). Notably, in March, May, and June 2023, Dunajec samples were slightly more enriched than those from S31 and S36. While such minor differences could be attributed to measurement uncertainty, sampling conditions may have played a role. In both March and June, samples were collected on rainy days, and on the days of sampling in May and June, relative humidity in Tarnów was low, at only 63% (IMWM-NRI, 2024) (Fig. S1). These conditions suggest that the slight enrichment in river samples may have resulted from the input of more enriched surface runoff and rainfall, as well as enhanced evaporation under lower humidity.

Between January and June 2023, the isotope signal in S37 and S39 showed less pronounced Dunajec influence than in the closer wells due to continuous native groundwater inflow. Their samples plotted along the water mixing line between Dunajec and E1 values, with S39 consistently closer to the river and S37 resembling native groundwater (Fig. 5). This difference likely reflects higher *K* values and shorter distance to the riverbank of S39 (Fig. 1; Table 1). The depleted δ-values in the Dunajec during meltwater-dominated months are consistent with upstream Dunajec and Poprad observations from March to June (Bodiš et al., 2015; Kotowski et al., 2023). At the southern Poland scale, the most depleted $\delta^{18}O$ and $\delta^{2}H$ values in recent Quaternary groundwaters occur in the Tatra Range macroregion (Fig. 7; Fig. S4), reflecting altitude and continental effects noted by Różański and Duliński (1988) and Leśniak and Wilamowski (2019). We must also note that the high contribution of meltwater from the Tatra Mountains to the Dunajec flow is also indicated by higher d-excess values, e.g. from February and March 2023, which is consistent with the observations of Sprenger et al. (2024), who showed that the d-excess of snowpack increase with elevation, which was directely reflected in stream water during the snowmelt/runoff season.

S1.3 Early July 2023 to early October 2023

Between 1 July and 3 October 2023, the Dunajec maintained elevated discharge (mean 74.8 $m^3\ s^{-1}$, max 471.6 $m^3\ s^{-1}$), driven by intense summer rainfall, especially in July and August (Fig. S1; Fig. S5–S6). Stable isotope data no longer indicated a meltwater contribution from July onward. $\delta^{18}O$ and $\delta^{2}H$ values in the river, as well as in S31 and S36, became notably enriched, with river samples exceeding native groundwater values in July and September (Fig. S2a–b).

Shallow native groundwaters in the Tarnów region reflect the long-term average isotopic composition of infiltrating precipitation (Fig. 5), showing relative stability compared to variable rainfall. In contrast, the Dunajec represents conditions from a specific hydrological year or season. This likely explains the shift of July and September river samples relative to E1 on the bivariate plot (Fig. 5). The enrichment observed in those samples was likely influenced by sampling during (July) or shortly after (September) intense rainfall events (Fig. S1) and/or by the partial evaporation due to high air temperature in the summer (Fig. S1). Rainfall at Kraków shows the highest $\delta^{18}O$ and $\delta^{2}H$ values from June to September (Duliński et al., 2019), supporting this interpretation. Elevated d-excess values in the river and Kraków precipitation in September 2023 further suggest a strong precipitation signal in the Dunajec recharge. As the July samples were collected during intense rainfall, enriched surface water had likely not yet reached S31 and S36, explaining their more depleted values relative to the river (Fig. 4). In September, S31 and S36 samples were more enriched than during the meltwater period and resembled native groundwater isotopically (Fig. 5). By October 2023, delta-values of the Dunajec, E1, S31 and S36 were closely aligned, with differences likely within measurement error, indicating substantial recharge of the river by regional groundwater and rainfall.

Samples from S37 and S39 showed minimal variation between July and October 2023, indicating limited river influence on their isotopic composition, in contrast to the pronounced seasonal response observed in S31 and S36. These findings support the conclusion that during low-flow periods without snowmelt contribution, the Dunajec is mainly recharged by regional groundwater, and the signal is directly reflected in the isotope values of S31 and S36. Therefore, regardless of the river's recharge sources at a given time, S31 and S36, due to their proximity to the riverbank, appear to represent the isotopic composition of the Dunajec reliably. This likely applies to the other five wells in an array closer to the river (Fig. 1).

The above findings support the broader inference that seven wells closer to the river may indicate water quality in the central and southern parts of the catchment. As such, they are potentially vulnerable to upstream surface water quality deterioration, particularly in the case of conservative contaminants. In contrast, S37 and S39, along with the two remaining wells located farther from the river (Fig. 1), abstract bank filtrate consistently mixed with native groundwater. As a result, the distinct seasonality, as well as the prominent Dunajec impact, are attenuated by the constant regional groundwater inflow from the landside, especially to the well S37.

S2 Contribution of river water and groundwater to production wells recharge

The results confirmed the Dunajec as the dominant recharge source for the production wells, particularly S31 and S36, where it contributed up to 100% of abstracted water based on $\delta^{18}O$, $\delta^{2}H$, Cl^{-}, and SC (Table S8). Similar contributions are likely in the other five wells near the river, given comparable distances and uniform geology across the RBF site (Fig. 1, Fig. 3). Mixing results for S37 and S39 were less consistent than for wells nearer the river. While Cl^{-} and stable water isotopes suggested greater river contribution to S39, SC indicated the opposite (Table S8). Notably, Cl^{-} suggested a higher Dunajec share than the isotopes, possibly due to elevated Cl^{-} levels in E1, located near a gas station, which may not reflect the natural regional background. This could lead to overestimating the river's influence on distant wells. Groundwater with lower Cl^{-} than in E1 may also contribute to recharge, potentially from the south, which is supported by a decrease in the Dunajec fraction in the models excluding the three months with the highest Cl^{-} values (Table S8). E1 samples from January to October 2023 averaged 78.4 mg L^{-1} (min = 63.1 mg L^{-1}; Table S3–S4). SC results suggested greater native groundwater input to S39 than S37, which may reflect unexamined processes along the flow path, such as ion exchange, mineral dissolution or precipitation, or redox reactions. Since SC reflects total ion concentration influenced by multiple constituents (U.S. Geological Survey, 2019), elevated values in the northern well field sector may indicate inflow of more contaminated or mineralised groundwater from the north-east.

Nevertheless, despite differences in tracer estimates, all four distant wells (Fig. 1) show a clear contribution from the Dunajec, likely greater in the site's northern part. Monthly data were also assessed for the memory effect (Table S8), observed for $\delta^{18}O$ in S31 and S36, $\delta^{2}H$ in all examined wells, and Cl^{-} in S37 and S39. The effect was most evident in river-proximal wells during transition periods when the Dunajec shifted from snowmelt-dominated to non-snowmelt conditions. For instance, in July 2023, water in S31 and S36 retained the isotopic signature of June, while the Dunajec had already shifted (Fig. S2a–b), indicating that a portion of water sampled in June remained in these wells and had not yet been fully exchanged.

The predominance of statistically non-significant results during non-meltwater periods (October–December 2022 and July–October 2023; Table S9) is notable. In such hydrogeological conditions, when the Dunajec resembles native groundwater due to dominant baseflow and rainfall contribution, at times even exceeding its $\delta^{18}O$ and $\delta^{2}H$ values (e.g. July and September 2023), determining individual end-member share becomes impractical due to their isotopic similarity. However, when these months were part of a broader dataset, including periods with stronger isotopic contrasts, EEMMA models still produced reliable results comparable to those for meltwater–dominated months alone. This suggests that limited sampling or datasets restricted to baseflow-dominant periods may lead to high standard errors and non-significant outcomes in the EEMMA analysis.

References

Bodiš, D., Krčmová, K., Cvečková, V., Rapant, S., Škoda, P., Slaninka, I., Michalko, J., Svasta, J., Grolmusová, Z., Mackových, D., Bystrická, G., and Antalík, M.: Geochemický Atlas Slovenskej Republiky. Časť VII. Povrchové Vody 1 : 1 000 000, (Geochemical Atlas Of The Slovak Republic. Part VII. Surface Waters 1 : 1 000 000. Bratislava: Štátny Geologický Ústav Dionýza Štúra, p. 110, ISBN 978-80-8174-014-5, 2015.

Falarz, M. (Ed.): Climate Change in Poland: Past, Present, Future, Springer International Publishing, Cham, https://doi.org/10.1007/978-3-030-70328-8, 2021.

IAEA/WMO: Global Network of Isotopes in Precipitation. The GNIP Database, https://nucleus.iaea.org/wiser, last access: 30 September 2024.

IMWM-NRI: Archival measurement and observation data belonging to the Institute of Meteorology and Water Management - National Research Institute. Data processed by the Authors, https://danepubliczne.imgw.pl/data/dane_pomiarowo_obserwacyjne/, 2024.

Janik, K., Ślósarczyk, K., and Sitek, S.: A study of riverbank filtration effectiveness in the Kępa Bogumiłowicka well field, southern Poland, J. Hydrol. Reg. Stud., 53, 101834, https://doi.org/10.1016/j.ejrh.2024.101834, 2024.

Kalvāns, A., Dēliņa, A., Babre, A., and Popovs, K.: An insight into water stable isotope signatures in temperate catchment, J. Hydrol., 582, 124442, https://doi.org/10.1016/j.jhydrol.2019.124442, 2020.

Kirchner, J. W.: eemma.R, an R script for Ensemble End-Member Mixing Analysis, , 46043 bytes, 501164 bytes, 4457 bytes, 1659 bytes, https://doi.org/10.16904/ENVIDAT.410, 2023.

Kotowski, T., Najman, J., Nowobilska-Luberda, A., Bergel, T., and Kaczor, G.: Analysis of the interaction between surface water and groundwater using gaseous tracers in a dynamic test at a riverbank filtration intake, Hydrological Processes, 37, e14862, https://doi.org/10.1002/hyp.14862, 2023.

Leśniak, P. M. and Wilamowski, A.: The δ 18 O and δD isoscapes of recent groundwater in Poland, Geologos, 25, 205–211, https://doi.org/10.2478/logos-2019-0022, 2019.

NASA Shuttle Radar Topography Mission (SRTM). Shuttle Radar Topography Mission (SRTM) Global. Distributed by OpenTopography. https://doi.org/10.5069/G9445JDF, 2013.

PGI-NRI: Data collected by the Polish Geological Institute – National Research Institute as part of the project "Updating and sharing information resources from the groundwater environmental tracers database". Unpublished data, not available publicly, made available at the authors' request, 2024.

Różański, K. and Duliński, M.: A reconnaissance isotope study of waters in the karst of the Western Tatra mountains, CATENA, 15, 289–301, https://doi.org/10.1016/0341-8162(88)90052-5, 1988.

Sitek, S., Janik, K., Jakóbczyk-Karpierz, S. (Ed.): Report on the desk analysis of the pilot feasibility study for MAR deployment in porous aquifers located near industrial sites on contamination of aquifers. https://programme2014-20.interreg-central.eu/Content.Node/DEEPWATER-CE/D.T3.4.1---DESK-ANALYSIS---PP4---FINAL.pdf, 2021.

Sprenger, M., Carroll, R. W. H., Marchetti, D., Bern, C., Beria, H., Brown, W., Newman, A., Beutler, C., and Williams, K. H.: Stream water sourcing from high-elevation snowpack inferred from stable isotopes of water: a novel application of d-excess values, Hydrology and Earth System Sciences, 28, 1711–1723, https://doi.org/10.5194/hess-28-1711-2024, 2024.

U.S. Geological Survey: Chapter A6.3. Specific Conductance, US Geological Survey, https://doi.org/10.3133/tm9a6.3, 2019.

Wojtal, G.: Hydrogeological documentation establishing exploitable groundwater resources of the groundwater intake Kępa Bogumiłowicka - wells S-30÷S-40 of Tarnów Waterworks Ltd. (in Polish), Tarnów Waterworks Ltd., 2009.